

# Centroid Based on Branching Contour Matching for 3D Reconstruction using Beta-spline

Normi Abdul Hadi, Arsmah Ibrahim, and Fatimah Yahya

Faculty of Computer and Mathematical Sciences, Universiti Teknologi MARA, 40450 Shah Alam, Malaysia

Email: {normi, arsmah, fatima}@tmsk.uitm.edu.my

Jamaludin Md Ali

School of Mathematical Sciences, Science University of Malaysia, 11800 Minden, Malaysia

Email: jamaluma@cs.my

**Abstract**—Reconstruction of real object often involves branching contour cases. An effective technique is required to determine the correct corresponding sub contour between two connected contours. This is to ensure the accuracy of the resulted image. This study has introduced a contour matching method using the similarity of the sub contour centroid value. The technique is fast enough equivalence to the requirement of reconstruction technique which has to be time and space effective. The matched sub contours then are connected by introducing an intermediate contour called as composite contour. The technique has been applied in the reconstruction of human head and Stanford bunny from CT images. Beta-spline was employed as the fitted surface as this surface has capability to give smoothed and accurate result.

**Index Terms**—branching contour, composite contour, centroid, Beta-spline

## I. INTRODUCTION

Branching contours is the case where the number of sub contours in the based contour different with the branched contours. Most of real objects especially in medical field contain the branching parts, and some of the objects contain more than one case of branching. Therefore, the 3-dimensional (3D) image reconstruction technique consumed must have capability to overcome this problem to produce an accurate result.

Branching contours always happen at the detail parts of an object. Human head and Stanford bunny for example, parts with branching contours are ears and nose. In ear part, cross section of the face has to be connected with the cross section of two ears. Same condition is applied in nose part where the lip has to be connected with two nose holes. The examples of ear and nose branching cases from human face are shown in Fig. 1 and Fig. 2.

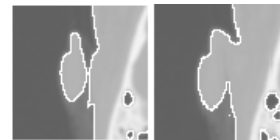


Figure 1. Many-to-one branching case in ear

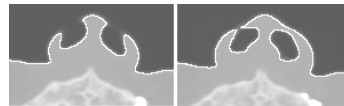


Figure 2. One-to-many branching case in nose

Images in Fig. 1 and Fig. 2 are from the Computerized Tomography (CT) scanner. The image was first in grey-level form and has been processed to extract the boundary of interest (BOI) as shown in Fig. 3 and Fig. 4.

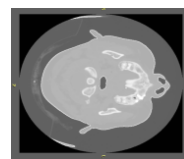


Figure 3. CT image



Figure 4. Binary form of CT image

In Fig. 3, the image consists of multi-level of intensity,  $I$ . Therefore, the image was simplified to only black and white pixel using a certain threshold,  $T$  as shown in (1).

$$I_{new} = \begin{cases} 1 & \text{for } I \geq T \\ 0 & \text{for } I < T \end{cases} \quad (1)$$

$T$  is calculated iteratively until the desired region is produced. The BOI is then extracted from the region. In Fig. 4, the BOI is extracted among the black pixels using  $3 \times 3$  technique as in Def. 1.

**Definition 1.** For each black pixel point,  $(i, j)$  it is a potential boundary point if any of its four neighbour pixels,  $(i+m, j+n)$ ,  $m=0, -1, 0, 1$   $n=1, 0, -1, 0$  is a white pixel.

From Def. 1, a black pixel point is set as a potential boundary point if at least one of its neighbour whether right, up, left or down is a white pixel [1]. The details of

the process can be referred in [2-3]. For human head cross section, the example of extracted BOI is in Fig. 5.

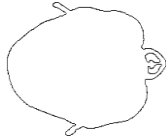


Figure 5. Extracted BOI of Fig. 4

The extracted BOI may have more than one contour. Fig. 5 is the example of a contour with three BOIs which are the cross sections of head, and two nose holes. This contour will be considered as branching case if it has to be connected with another contour with different number of sub contours.

Branching contours case can be generally categorized into many-to-one (or one-to-many), many-to-many and no link cases. The examples of these cases are shown in Fig. 6 to Fig. 8.

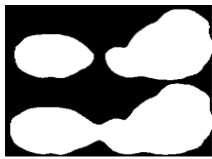


Figure 6. One-to-many case

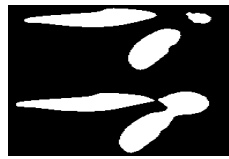


Figure 7. Many-to-many case



Figure 8. No-link case

Fig. 6 is a one-to-many case where the shape of base contour is obviously dissimilar with both sub contours in the branch. Fig. 7 is a many-to-many case where two sub contours in the base have to be connected with three sub contours in the branch. In this case, the correspondence sub contour has to be correctly determined. Same condition applied in Fig. 8 case which is the example of no-link case. In this figure, the number of sub contours in the base is greater than then the number of sub contours in the branch. Thus, a sub contour in the base has no correspondence contour.

Each branching case is solved within two consecutive contours called as base and branched contours. In connecting these contours, the correspondence sub contour has to be properly recognized to ensure the correctness of the reconstructed surface and avoid twisted surface as shown in Fig. 9 and Fig. 10.

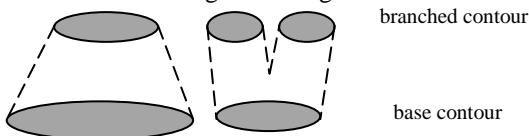


Figure 9. Right connections between base and branched contours

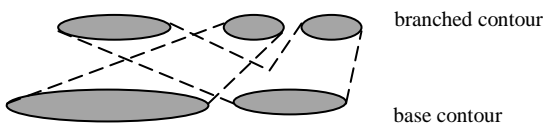


Figure 10. Wrong connections between base and branched contours

Fig. 9 is the example of right connection between two base sub contours and three branched sub contours. However, Fig. 10 shows the twisted surface produces if these contours are imperfectly connected.

The effective technique to identify which sub contour belongs to which sub contour is using the similarity between both of them. This similarity can be determined whether visually or computationally with associated parameters. However, visual comparison is not suggested as naked-eyes technique is not reliable.

Contour matching is a process to evaluate the similarity and dissimilarity degree between two images in order to align or classify the image [4]-[5]. It is mostly used in image recognition and classification such as in letter [6]-[7] and face recognition, and defect [8]-[9] and biometric [4] classifications. The similarity between two images is based on the extracted information of the image whether in geometric or non-geometric forms. For geometric based classification, the features are such as gradient value of contour points [6], the distance between corner points to the image centroid [4], [10], area, and perimeter. The information then is structured and used to measure the similarity of the images. The intensity of each image boundary point can also be one of the image information, but it is for non-geometric based classification.

In 3D reconstruction, contour matching is the contour alignment process to ensure the correct connection between base and branched contours. This process is not the main focus in the reconstruction, thus a fast and accurate technique is required. Moreover, the comparison is done between two contours, not from a database as for image recognition. Therefore, this study has proposed a method to determine the corresponding contour from base to branched contours based on the contour centroid. The method is discussed in section II. Section III shows the composite contour generation between base and branched contours. The fitted Beta-spline surface is shown in section IV. This paper ends with conclusion in section V.

## II. CENTROID BASED CONTOUR MATCHING

Centroid is the average of all position of boundary points,  $P_i = (x_i, y_i)$  [11].

$$\text{Centroid} = \frac{\sum_i^N P_i}{N} \quad (2)$$

Since the centroid is in  $(x, y)$  form, the value shows the position of the sub contour in Cartesian coordinate. Thus, the centroid is suitable to be used in detecting the corresponding sub contour from the adjacent slice since the corresponding sub contours commonly have same location in the whole contour. The considered CT images in this study are not rotated or scaled which may change the centroid value.

Centroid  $C_i$  for each sub contour  $S_i$  is calculated for both base and branched contours and labeled as  $C_i^{ba}$ ,  $C_j^{br}$ ,

$S_i^{ba}$  and  $S_j^{br}$  respectively. Each calculated  $C_i^{ba}$  is then compared with all calculated  $C_j^{br}$  and error  $e_i^j$  is evaluated. Certain value of  $e_i^j$  shows that sub contour  $S_i^{ba}$  with centroid  $C_i^{ba}$  is matched with sub contour  $S_j^{br}$  with centroid  $C_j^{br}$ . Detail on error calculation is discussed in section III. The examples of several contours from Stanford bunny are shown in Table I.

TABLE I. CENTROID CALCULATION FOR STANFORD BUNNY CONTOURS

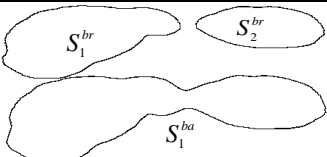
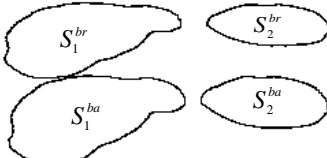
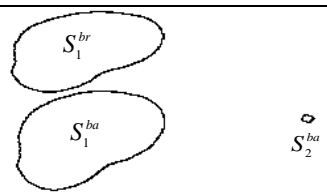
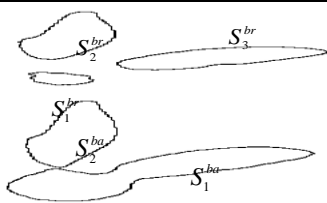
Case	Contours	Centroid
One-to-many	 <p>Figure 11. One-to-two case</p>	$C_1^{br} = (209.565, 171.735)$ $C_2^{br} = (100.894, 157.445)$
		$C_1^{ba} = (165.930, 165.937)$
Many-to-many ( $i = j$ )	 <p>Figure 12. Two-to-two case</p>	$C_1^{br} = (209.565, 171.735)$ $C_2^{br} = (100.894, 157.445)$
		$C_1^{ba} = (211.079, 172.491)$ $C_2^{ba} = (100.894, 157.445)$
Many-to-one	 <p>Figure 13. Two-to-one case</p>	$C_1^{br} = (216.807, 174.874)$
		$C_1^{ba} = (217.249, 174.970)$ $C_2^{ba} = (95.039, 158.538)$
Many-to-many ( $i \neq j$ )	 <p>Figure 14. Two-to-three case</p>	$C_1^{br} = (214.714, 170.661)$ $C_2^{br} = (213.809, 76.886)$ $C_3^{br} = (172.129, 131.945)$
		$C_1^{ba} = (170.021, 130.035)$ $C_2^{ba} = (213.636, 74.104)$

Fig. 11 is a one-to-many case where the shape of  $S_1^{ba}$  is totally different with  $S_1^{br}$  and  $S_2^{br}$ . In Fig. 12, both  $S_1^{ba}$  and  $S_2^{ba}$  have respective corresponding sub contours in the branch. However, the correct connection has to be determined to avoid twisted surface as shown in Fig. 10 before. Fig. 13 and Fig. 14 also have similar contours for example  $S_1^{ba}$  and  $S_1^{br}$  in Fig. 13 and  $S_2^{ba}$  and  $S_2^{br}$  in Fig. 14. For  $S_2^{ba}$  in Fig. 13, it is a no-link case, and  $S_1^{ba}$  in Fig. 14 is the same case as Fig. 11 which

has to be connected with  $S_1^{br}$  and  $S_3^{br}$ . The decision of which branching case the contour belongs to is decided using the similarity.

The similarity between the two contours can be visually seen from the shape of the contours or determined using the its geometrical features. In this study, the similarity is proposed to be decided by comparing the centroid values from both contours. A sub contour from base can be matched to a sub contour in the branch if the error between two centroids is below a certain threshold. The errors for matching sub contours in Fig. 11 to Fig. 14 are displayed in Table II.

TABLE II. ERROR BETWEEN BASE AND BRANCHED SUB CONTOURS CENTROID

Fig.	Compared Sub contours	Error	Matched
11	$C_1^{ba} - C_1^{br}$	44.019	
	$C_1^{ba} - C_2^{br}$	65.588	
12	$C_1^{ba} - C_1^{br}$	1.692	√
	$C_1^{ba} - C_2^{br}$	111.208	
13	$C_2^{ba} - C_1^{br}$	109.607	
	$C_2^{ba} - C_2^{br}$	0	√
14	$C_1^{ba} - C_1^{br}$	0.496	√
	$C_2^{ba} - C_1^{br}$	122.859	
14	$C_1^{ba} - C_1^{br}$	60.398	
	$C_1^{ba} - C_2^{br}$	68.864	
	$C_1^{ba} - C_3^{br}$	2.845	
	$C_2^{ba} - C_1^{br}$	96.563	
14	$C_2^{ba} - C_2^{br}$	2.787	√
	$C_2^{ba} - C_3^{br}$	71.193	

From the calculated error, the sub contours are said to be matched if the error between both contours is within a certain range. Result in Table II shows that the suitable error range for the case is from 0 to 2.787. Using this range, it is suggested that no matched sub contours for Fig. 11,  $S_2^{ba}$  in Fig. 13 and  $S_1^{ba}$  in Fig. 14. This is because Fig. 11 and  $S_1^{ba}$  in Fig. 14 are the one-to-many case, and  $S_2^{ba}$  in Fig. 13 is the no-link case. Thus, the calculated error gives the idea whether the sub contour has one-to-one case with corresponding match, or else. This error range will change if more branching case is considered.

In some case as happened in  $C_1^{ba} - C_3^{br}$  in Fig. 14, the error is 2.845 which closed to the maximum error range 2.787. Thus, additional step is required to support the idea that  $C_1^{ba} - C_3^{br}$  is unmatched. Another suitable similarity is using the area of the sub contour region. The areas of  $S_1^{ba}$  and  $S_3^{br}$  for Fig. 14 are 2703 unit<sup>2</sup> and 1524 unit<sup>2</sup> respectively.

The calculated areas of  $S_1^{ba}$  and  $S_3^{br}$  have big different and show dissimilarity between both sub contours.

Finally, after matched sub contours have been determined, surface is fitted into these contours easily since it is one-to-one case. For many-to-one and no-link case, other methods are applied before the surface fitting procedure.

In no-link case as occurs in  $S_2^{ba}$  in Fig. 13, the sub contour is matched to its own centroid value. This is to ensure this sub contour has closed surface. This case is also called as capped case where the sub contour has to be capped. For many-to-one or one-to-many case, the case is reduced to one-to-one case before the surface is fitted. A new intermediate contour called as composite contour is inserted between base and branched contours and discussed in section III.

### III. COMPOSITE CONTOUR GENERATION FOR BRANCHING CONTOURS

Composite contour is a new contour inserted between base and branched contours. The height level of this contour is  $z_{composite}$ , where

$$z_{composite} = \frac{z_{base} + z_{branched}}{2} \quad (3)$$

This intermediate contour is used to simplify the not many-to-one or one-to-many branching case as shown in Fig. 15.

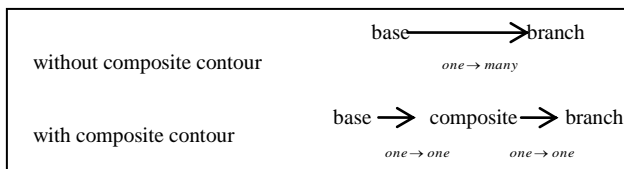


Figure 15. Simplification of branching case using composite contour

Fig. 15 shows the way that composite contour has reduced a one-to-many branching case to two cases of one-to-one.

Initially, the data points in the composite contour are the points of base and branched contours. Then, points are modified using the midpoint  $e_i$ .

Let the branched data points as  $P_i^{br}$ , and the base resampling points as  $R_j^{ba}$ . For each  $R_j^{ba}$ ,  $D_j^{ba}$  is the shortest distance from  $R_j^{ba}$  to the branched at point  $P_i^{br}$ , and  $D_j^{br}$  is the shortest distance from  $R_j^{ba}$  to other base sub contours. Then, midpoint  $e_i$  is calculated for  $D_j^{ba} < D_j^{br}$ .

Resampling point,  $R_j^{ba}$  is the curve point extracted at parameter  $t_j$ , where

$$t_j = j \times h \quad (4)$$

$h$  is the required interval between the points, where

$$h = \frac{\text{total contour length, } L}{\text{required number of resampling point}} \quad (5)$$

$L$  is the total contour length calculated as,

$$L = \int_0^1 \sqrt{x'(t)^2 + y'(t)^2} dt \quad (6)$$

The stacked form of the base, branch and composite contours of Fig. 11 case are shown in Fig. 16. The details of the composite contour generation process can be read in Ref. [12]-[13].

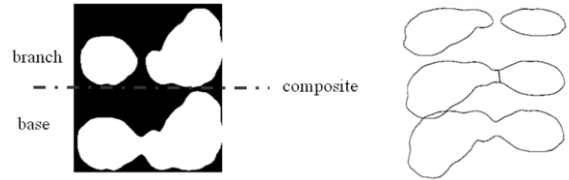


Figure 16. Base, branched and composite contours

After the composite contour is generated, surface is fitted using one-to-one technique. The surface fitting process using Beta-spline is discussed in the next section.

### IV. BETA-SPLINE SURFACE FITTING OF CONTOURS

Basis equation of cubic Beta-spline surface is a tensor product where,

$$F(t, u) = \sum_{i=0}^3 \sum_{j=0}^3 V_{i,j} b_i(t) b_j(u) \quad (7)$$

With a set of  $4 \times 4$  control points matrix  $V_{i,j}$  and basic functions  $b_i(t)$  and  $b_j(u)$  as,

$$\begin{bmatrix} b_0(t) \\ b_1(t) \\ b_2(t) \\ b_3(t) \end{bmatrix}^T = \begin{bmatrix} t^3 & t^2 & t & 1 \\ -2\beta_1^3 & 2(\beta_2 + \beta_1^3 + \beta_1^2 + \beta_1) & -2(\beta_2 + \beta_1^2 + \beta_1 + 1) & 2 \\ 6\beta_1^3 & 3(\beta_2 + 2\beta_1^3 + 2\beta_1^2) & 3(\beta_2 + 2\beta_1^2) & 0 \\ -6\beta_1^3 & 6(\beta_1^3 - \beta_1) & 6\beta_1 & 0 \\ 2\beta_1^3 & \beta_2 + 4(\beta_1^2 + \beta_1) & 2 & 0 \end{bmatrix} \quad (8)$$

$$\delta = \beta_2 + 2\beta_1^3 + 4\beta_1^2 + 4\beta_1 + 2 \quad (9)$$

The control points are the resampling points extracted as in (4) to (6). The developed branching techniques are applied into human head and Stanford bunny data. The examples of human head and Stanford bunny in wireframe form are shown in Fig. 17 and Fig. 18.

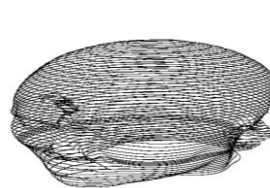


Figure 17. Wireframe of human head

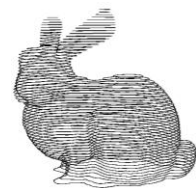


Figure 18. Wireframe of Stanford bunny

Beta-spline is chosen due to its capability to give an accurate and  $G^2$  continuous although the new contour has been inserted. The reconstructed human head and

Stanford bunny using Beta-spline surface are shown in Fig. 19 and Fig. 20.



Figure 19. Reconstructed human head using Beta-spline

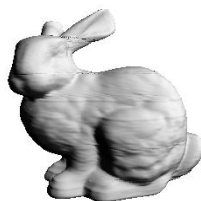


Figure 20. Reconstructed Stanford bunny using Beta-spline

The use of composite contour also makes the reconstruction objects separated into several parts according to the number of composite contours. In Stanford bunny for example, it is divided into four main parts: body, back, head, and ears as shown in Fig. 21 to Fig. 24.

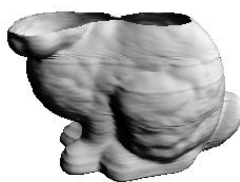


Figure 21. Body



Figure 22. Head



Figure 23. Back



Figure 24. Ears

Composite contour generation process as shown in Fig. 15 has produce the body, head, and back parts. These parts are not connected to each other. Thus, the number of resampling points for each part can be different associated with the part size. Body part for example is larger than back part. Therefore, the number of resampling points of body should be larger than the back. This method also can reduce the storage and time usage since the number of resampling point can be reduced.

## V. CONCLUSION

A fast and accurate technique for contour matching process of branching contour case is proposed. The technique is the comparison of centroid value of sub contours in base and branched contours respectively. Besides the comparison of centroid, other geometric features can also be used such as area, perimeter, and elongation. The error result shows the reliability of this method in determining the matched contours of base and

branch. However, the calculation of error range in determining the matched sub contours should be improved to ensure the effectiveness of the technique.

## ACKNOWLEDGMENT

This study is supported by Ministry of Higher Education, and Universiti Teknologi MARA, Malaysia.

## REFERENCES

- [1] M. Sarfraz and A. Masood, "Capturing outlines of planar images using Bézier cubics," *Computers & Graphics*, vol. 31, pp. 719-729, 2007.
- [2] N. A. Hadi, A. Ibrahim, F. Yahya, and J. M. Ali, "Beta-spline Surface Fitting to Multi-slice Images," *Journal of World Applied Science and Technology*, pp. 1326-1331, 2012.
- [3] N. A. Hadi, A. Ibrahim, F. Yahya, and J. M. Ali, "3-Dimensional Beta-spline wireframe of human face contours," in *Proc. IEEE 8th International Colloquium on Signal Processing and its Applications*, 2012, pp. 110-114.
- [4] H. Li, Z. Guo, S. Ma, and N. Luo, "A New Touchless Palmprint Location Method Based on Contour Centroid," in *Proc. International Conference on Hand-Based Biometrics*, 2011, pp. 1-5.
- [5] I. Y. Liao, P. Zheng, and B. Belaton, "Skull registration using rigid super-curves," in *Proc. Sixth International Conference on Computer Graphics, Imaging and Visualization*, 2009, pp. 475-479.
- [6] Y. Pourasad, H. Hassibi, and M. Banaeyan, "Persian characters recognition based on spatial matching," *World Applied Sciences Journal*, vol. 13, pp. 239-243, 2011.
- [7] H. Aboaisa, Z. Xu, and I. El-Feghi, "An investigation on efficient feature extraction approaches for Arabic letter recognition," in *Proc. Queen's Diamond Jubilee Computing and Engineering Annual Researchers' Conference*, 2012, pp. 80-85.
- [8] S. A. Halim, N. A. Hadi, A. Ibrahim, and Y. Manurung, "The geometrical feature of weld defect in assessing digital radiographic image," in *Proc. IEEE International Conference on Imaging Systems and Techniques*, 2011, pp. 189-193.
- [9] L. Y. Fang, H. Li, and J. P. Bai, "Defect contour matching based on similarity measure for 3D reconstruction," *Advanced Materials Research*, vol. 308, pp. 1656-1661, 2011.
- [10] F. P. M. Oliveira and J. M. R. S. Tavares, "Matching contours in images through the use of curvature, distance to centroid and global optimization with order-preserving constraint," *FEUP-Artigo em Revista Científica Internacional*, 2009, pp. 91-110.
- [11] Q. Zhou and J. K. Aggarwal. (2001). Tracking and classifying moving objects from video. [Online]. Available: <http://read.pudn.com/downloads155/doc/688112/Tracking%20and%20classifying%20moving%20objects%20from%20video.pdf>
- [12] J. H. Ryu, H. S. Kim, and K. H. Lee, "Contour-based algorithms for generating 3D CAD models from medical images," *International Journal of Advanced Manufacturing Technology*, vol. 24, pp. 112-119, 2004.
- [13] N. A. Hadi, A. Ibrahim, F. Yahya, and J. M. Ali, "Composite contour generation for Beta-spline surface reconstruction," presented at the 20th National Symposium on Mathematical Sciences, Malaysia, 2012.

**Normi A. Hadi** is a lecturer in Mathematics department of Universiti Teknologi MARA, Malaysia. The author is a member of Malaysian Mathematical Sciences Society, and Geometric Surface Design research group. The research interest is in curve and surface fitting process especially in medical images.